World Academy of Science, Engineering and Technology
International Journal of Energy and Power Engineering
Vol:11, No:3, 2017

Analysis of Thermoelectric Coolers as Energy Harvesters for Low Power Embedded Applications

Yannick Verbelen, Sam De Winne, Niek Blondeel, Ann Peeters, An Braeken, Abdellah Touhafi

***Abstract*—**The growing popularity of solid state thermoelectric devices in cooling applications has sparked an increasing diversity of thermoelectric coolers (TECs) on the market, commonly known as "Peltier modules". They can also be used as generators, converting a temperature difference into electric power, and opportunities are plentiful to make use of these devices as thermoelectric generators (TEGs) to supply energy to low power, autonomous embedded electronic applications. Their adoption as energy harvesters in this new domain of usage is obstructed by the complex thermoelectric models commonly associated with TEGs. Low cost TECs for the consumer market lack the required parameters to use the models because they are not intended for this mode of operation, thereby urging an alternative method to obtain electric power estimations in specific operating conditions. The design of the test setup implemented in this paper is specifically targeted at benchmarking commercial, off-the-shelf TECs for use as energy harvesters in domestic environments: applications with limited temperature differences and space available. The usefulness is demonstrated by testing and comparing single and multi stage TECs with different sizes. The effect of a boost converter stage on the thermoelectric end-to-end efficiency is also discussed.

***Keywords*—**Thermoelectric cooler, TEC, complementary balanced energy harvesting, step-up converter, DC/DC converter, embedded systems, energy harvesting, thermal harvesting.

I. Introduction

SOLID state thermoelectric devices have a long history of being used for cooling purposes [12] in applications where size is a more important factor than thermoelectric efficiency [48], [17]. These thermoelectric coolers (TECs) are also appreciated for their silent cooling capabilities in stealthy applications, as opposed to noisy pumps and fans. Integration in consumer products has increased demand and fuelled their large scale production in recent years, in turn decreasing their price and allowing them to spread outside the specialized market segments they were originally used in [24], [34]. The combination of decreasing prices and better availability have opened opportunities in new domains, including low power electronics as energy harvesters [33]. Traditional solid state thermoelectric coolers are entirely bidirectional from a thermoelectric perspective because of the Seebeck effect on which they rely, and can be used both as cooling devices or as thermoelectric generators (TEGs). When a temperature difference is applied to a junction of two materials with a different thermoelectric constant, a small potential difference will be created over this junction [9]. The voltage is a function of the thermoelectric materials being used, and the temperature difference that is applied. As heat flows through the device from the 'hot' side of the junction to the 'cool' side, a heat flux is effectively converted into electric power [4]. The maximum thermodynamic power available [14] is given by

$$P_{max} = \frac{\Delta T^2}{4T_0(K_c + K_h)} \tag{1}$$

For thermoelectric generators, the heat flux to electric power conversion depends on the Seebeck coefficient S, the thermal conductivity κ, the electrical conductivity σ and the temperature difference ΔT (1) [12], and can be approximated as the dimensionless figure of merit zT [13], [17, p. 190]:

$$zT = \frac{S^2 \Delta T}{\sigma \kappa} \tag{2}$$

Higher Seebeck coefficient and temperature difference, and better thermal and electrical conductivity of the material, will result in better heat flux to power conversion. The figure of merit zT as shown in (2) is a parameter of thermoelectric efficiency. Although zT is straight forward to model, the thermal (κ) and electrical (σ) conductivity of thermoelectric materials is difficult to measure, especially at elevated temperature differences [13], because of the Thomson effect [22], [7]. The design and simulation of accurate models for thermoelectric generators [26] is subject of ongoing research efforts [14], [17], and advanced modeling efforts have resulted in sophisticated models [37], [27]. These models unfortunately rely on an extensive set of parameters [27, p. 188, Table 1] which are not easily obtained for the commercial thermoelectric generators that are typically integrated in electronic devices for energy harvesting purposes. A second uncertainty is the physical construction of the TEG, including but not limited to the ceramics used as contact surface, insulating materials, and of course the thermoelectric junctions themselves. For bismuth telluride (Bi_2Te_3), the thermal conductivity κ is 1.6 W/mK for example [7], but values strongly differ between materials. Many thermoelectric materials have been used to construct TEGs, of which PbTe [8], [19] and Bi_2Te_3 [5], [16] are the most common. Other materials with high zT are Mg_2Si [49], PbSnTe [2], $AgPbSbTe_2$ [21], $Yb_{14}MnSb_{11}$ [3], $CeFe_4Sb_{12}$ [38], $FeSi_2$ [47], SiGe [39], InGaAs [2], and recently also perovskite and graphene [46].

Current research focuses on making better use of existing materials by means of performance optimization through nanotechnology [15] and MEMS structures [20], rather than discovering new materials with an even higher figure of merit.

Yannick Verbelen is with the Vrije Universiteit Brussel, Pleinlaan 2, 1050 Etterbeek, Brussels, Belgium (corresponding author, e-mail: yannick.verbelen@vub.ac.be).

Sam De Winne, Niek Blondeel, Ann Peeters, An Braeken and Abdellah Touhafi are with the Vrije Universiteit Brussel, Pleinlaan 2, 1050 Etterbeek, Brussels, Belgium.

The relative rarity of some of the raw materials currently required for TEG construction are pushing towards perovskite and graphene, causing the market to grow more diverse as the share of traditional Bi_2Te_3 TEGs drops [46], [5]. As of 2016, Bi_2Te_3 TEGs are still the most widely used type, however. From the perspective of an embedded systems designer, looking to make use of TEGs as a replacement for primary chemical cells in electronic applications, the complexity of TEG operation at a fundamental physical level prohibits straight-forward integration. The lack of sufficiently detailed datasheets [12] and the necessity of a power conversion stage between TEG and electronic system [36] are posing serious barriers to large scale TEG adoption. The large variety of semiconductor materials that may be used in TECs, and the performance dependence on specific construction details (i.e. material depositing techniques, thin film, MEMS etc.) make theoretical performance predictions a difficult and research intensive task. Currently, many applications make use of reference designs based on case studies [36], which are most likely suboptimal for other applications [34]. A better method for testing the performance of commercial TECs as energy harvesters is therefore necessary.

In this article, the design and implementation of an automated test setup for TEGs is presented that allows easy analysis of commercial thermoelectric cooler performance in real world environments, thereby eliminating the need for extensive parameter sets or complex thermodynamic models. The presented test setup allows to characterize TEG performance in combination with power path circuitry to provide accurate estimations of TEG performance in low ΔT environments. In Section II, existing test setups for high power TEGs are discussed, from which the specifications for our implementation are derived in Section III. Section IV presents an overview of the system, and Section V proceeds with the verification of the design to demonstrate its use. Finally, Section VI compares the performance of commercial TECs with and without a DC/DC boost stage, and the article concludes with the proposal of several future adjustments and modifications in Section VII.

II. Previous Work

Several test setups for measuring TEG performance have been suggested by other authors as an alternative to TEG simulation [26]. Most of these implementations focus on higher power TEGs [41], such as for automotive waste heat recovery. Ahiska and Mamur make a comparison of test setup performance based on temperature differences and power measurements [1, p. 16]. Their PLC controlled implementation complicates automated testing, however. Montecucco et al. present their approach in [29], and it is capable of measuring the TEG's maximum power point (MPP) by varying the load. The authors allow a maximum temperature up to 800 °C, not usually present in domestic environments. Up to 4 TEGs can be measured at once. The primary advantage of the setup presented by Montecucco et al. is its independence of physical or electrical parameters. Niu et al. present a water cooled approach, using a variable resistor as load [32, p. 622], as opposed to the Peltier cooling presented by Faraji and Akbarzadeh [12, Fig. 1]. Carmo et al. use forced air cooling for lower temperature differences [6, p. 2197], in combination with a hot plate to heat the hot side. Synergy with the power conversion stage is necessary, however. Laird et al. discuss MPP algorithms and present an implementation using a PWM controlled IGBT in a synchronous buck topology as variable load [25, p. 56]. In [30, p. 5] a similar topology is used based on an N-channel MOSFET instead of IGBT. Both systems focus on high power ratings, necessitating switched system topologies, and a snubber network may be required [30, p. 7] to compensate for parasitic inductances between TEG elements. A SEPIC topology may also be used [10, p. 693]. Linear topologies are also documented in literature: Muller et al. present a switchable resistor bank in [31]. Alternatively, an IGBT [43] or MOSFET [42] can be used in its finite impedance region as linear electronic load. A varying degree of control has also been implemented by previous authors: PLC [1] and microcontroller [10, p. 698], [43], [42] are the most common, but more simple systems without software control also exist [23, p. 1541]. Since for energy harvesting purposes the power rating is low ($P < 100$ mW) compared to the maximum power that can be dissipated in a typical power MOSFET or IGBT ($P > 5$ W), a linear approach as documented by Van Belle in [42] was chosen.

III. Operation Range and Requirements

Depending on the physical construction of the junction, the voltage over a common Bi_2Te_3 TEC junction can be expected between -228 μV/K [50, p. 85] and -287 μV/K [40]. As a material with relatively high zT [17], still a significant number of junctions must be thermally placed in parallel but electrically in series to generate a useful voltage. As a result, in order to be practically usable, either a large surface (i.e. more elements in series) or a large temperature difference is required for practical operation. Fortunately, as embedded electronic devices are improving, their power requirements and operating voltages are also dropping [44]. That is particularly for TEG powered applications a favourable evolution: Less power conversion circuitry will be required, and the electrical conversion efficiency will be higher [45]. It also allows representative testing of TEGs and their power conversion circuitry together, resulting in power figures that are more accurate than measuring the TEG output with MPP and the power circuitry separately. For this research we primarily focused on Bi_2Te_3 TEGs since they are the most widely available commercial heat flux energy harvesters and have good performance [41]. However, it should be noted that other TEG types may be better suited for complementary balanced energy harvesting applications [46]. For use in domestic applications, industrial temperatures as in [29] are never reached, and thus a maximum high side temperature of 100 °C (boiling water) was chosen as upper limit, since this is the maximum temperature that can commonly be achieved in office or home heating appliances without pressurization. For the same reason, since active 'cold' sources are rare in conjunction with heat sources, we will focus on ambient air

cooling instead of forced cooling. A heat sink will be used for this purpose. Considering an average indoor temperature between 20 °C for office buildings and 22 °C-25 °C for home environments, the maximum temperature difference considered is ca. 80 °C. However, this assumes the heat sink would be able to keep the cold side of the TEG at room temperature, which would require the heat sink to be impractically large. Since 3.3 V power rails are standard for low power embedded devices, a maximum voltage of 5 V was chosen for harvester/power conditioning circuitry output.

IV. System Overview

The system consists of 3 major parts: A heated bed of 25 cm by 25 cm with integrated temperature sensor (1), a heat sink with optional forced air cooling using a fan (2) and a control unit for data acquisition and communication with a computer (3), as seen in Fig. 1. Heat sink and heated bed are monitored with an industry standard LM35 temperature sensor from Texas Instruments (Fig. 1, insert), and the heating power is modulated to achieve a desired temperature difference over the TEG being tested (DUT). For higher temperature differences, passive cooling is not sufficient at room temperature for TEGs with a good thermal conductivity, and forced air cooling with a fan may be necessary to maintain the temperature difference. Temperature stabilization is implemented with a PID controller in software on a PIC24F16KA102 microcontroller from Microchip.

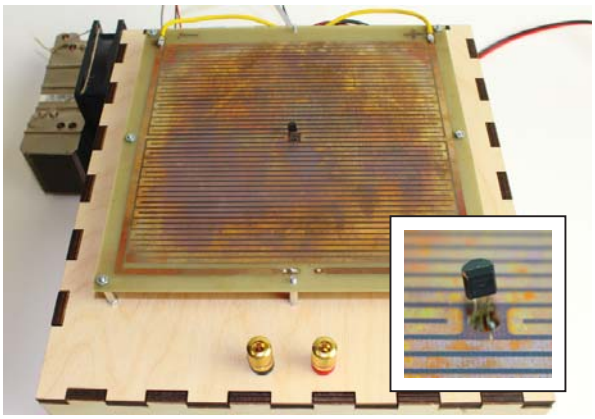

Fig. 1 Heated bed constructed with a PCB trace on standard 1.6 mm FR4 as planar resistor. TEG and forced air cooled heat sink are dismounted, heat sink visible on the left of the setup. Insert: A close-up of the LM35 temperature sensor monitoring the hot side of the TEG, fitting into a cavity of the ceramic plate (not shown) on which the TEG is mounted

The microcontroller reads the temperature of hot and cold side of the TEG, computes the temperature gradient ΔT and adjusts the heated bed power to increase or decrease the temperature on the hot side if necessary. The temperature difference is considered stable if 150 successive measurements fall within an error margin of ± 1 °C. The accuracy is limited by the LM35, causing a larger error on measurements at low temperature gradients, as seen in Fig. 2.

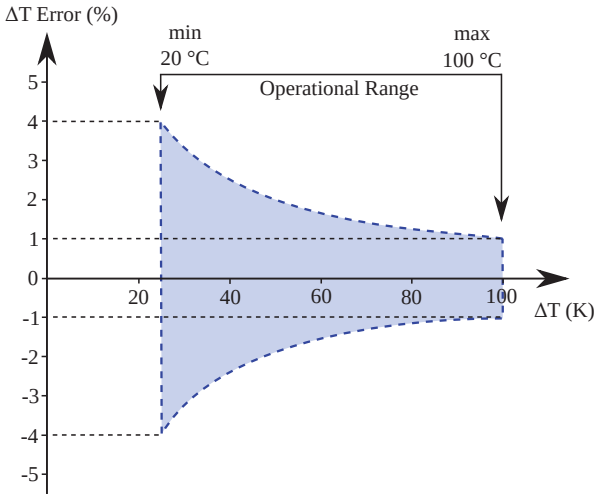

Fig. 2 Relative error on the temperature measurement over the operational range between room temperature

A. Power Measurements

When a stable temperature gradient is reached, the data acquisition (DAQ) module is notified to measure output voltage and current. To ensure optimal stability and eliminate any interference between control and DAQ, measurements are performed by a separate microcontroller, also of type PIC24F16KA102. The current is measured over a 100 mΩ shunt resistor using an INA226 high side current/power monitor. In the INA226, the voltages on each side of the shunt resistor are fed to an integrated analog to digital converter (ADC) separately and then subtracted rather than using an analog differential amplifier topology. The advantages are twofold: the device can be used for both high and low side measurements (i.e. load connected to power rail or to ground), and the load voltage is measured simultaneously with the current, allowing direct computation of output power. The INA226 thus acts as a 4 wire sensing device. The primary reason for choosing an ADC with integrated switch is the better noise immunity in comparison to topologies with separate differential amplifier and ADC stages. The SMbus/I^2C interface also allows easy interfacing with the microcontroller responsible for DAQ, and ensures the measured power reaches its 0.1 % gain error and 10 μV offset specs. The electrical connectivity diagram is shown in Fig. 3.

B. Maximum Power Point Tracking

For maximum power point tracking (MPPT), the perturb & observe algorithm has been implemented. By sweeping the load between open circuit voltage (V_{oc}) and short circuit current (I_{sc}), the UI-curve of the TEG can be obtained, which allows to compute the maximum power point. The variable load has been implemented with a linear drive of an N-channel MOSFET [42] of type IRF540 from International Rectifier (IR). However, instead of using a passive filter to control the MOSFET as in [42], a digital to analog converter (DAC) of type MCP4921 from Microchip was chosen instead because of its better transient response and stability. The non-existing

ripple also simplifies the feedback loop and allows it to be implemented in software on the same microcontroller that is doing the DAQ. Current/power measurements do not interfere with stabilization because the INA226 is connected over I^2C while the DAC uses a faster SPI connection, as shown in Fig. 3. The output of the DAC is compared to the drain voltage of the MOSFET with an OPA1644 opamp so that the channel impedance is adjusted to match the voltage over the channel with the MCP4921 output voltage.

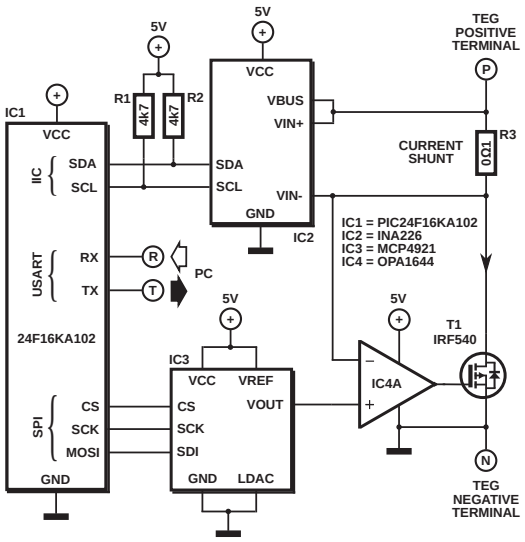

Fig. 3 Schematic diagram of the DAQ module, showing digital control (PIC24F16KA102), a current sense amplifier (INA226) connected over I^2C, and a DAC (MCP4921) connected over SPI. A local feedback loop is implemented with a OPA1641/OPA1644A opamp as direct MOS driver

The voltage drop over the current shunt resistor does not have to be compensated for because it is measured by the INA226 and can thus be subtracted in the software feedback loop. Feedback from the high side (VIN+) is not possible with INA226 because it is unable to measure the voltage on the high side separately. Therefore, feedback from the low side (VIN-) has been implemented.

C. Control Logic

Both PIC24F16KA102 microcontrollers are interfaced with a computer over a USB connection with CDC driver to implement a virtual UART connection using an MCP2200 integrated I/O controller. The software on the computer side is written in C#, and responsible for temperature stabilization and data management. The control loop first stabilizes the TEG at the desired temperature difference and waits until 150 successive measurements indicate time invariance. When stable, the power measurement is then started following the procedure presented above. After completing sufficient measurements to generate an UI-curve, the software renders the data points and saves them to disk.

V. Design Verification

To verify the proposed topology, a verification setup was constructed using a lab power supply with current control functionality. The output voltage of this PSU remains constant regardless of the load, but drops sharply to zero when a configurable current limit is exceeded. the output voltage was set to 4.63 V and the current limit to 119.2 mA, arbitrary values within the range of the test setup that could easily be verified with a precision multimeter. This is the MPP of the supply. As a result, the expected maximum current of 119.2 mA and 0 V output voltage occurs when the load is $\pm 0\ \Omega$, corresponding to the short circuit current I_{sc}.

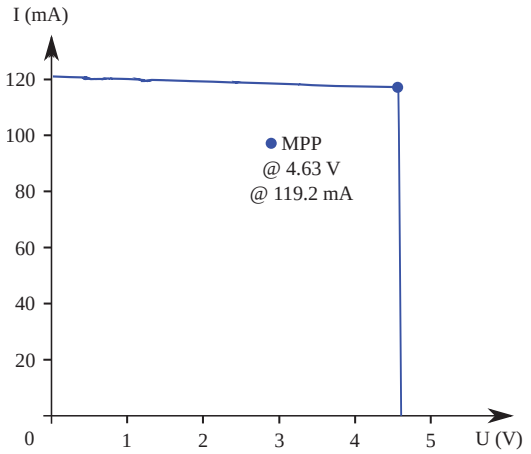

Fig. 4 Maximum power point tracking on a regulated bench top power supply. As long as the voltage set point (4.63 V) is not reached, the power supply will drive the maximum short circuit current (119.2 mA)

When the load is subsequently decreased by increasing the load impedance, the output current remains at 119.2 mA but the voltage will climb proportional to Ohm's Law. When the MPP of the supply is reached, the current will drop while the voltage remains at its set point, 4.63 V in this case. Fig. 4 shows the measurement, which meets the expectations.

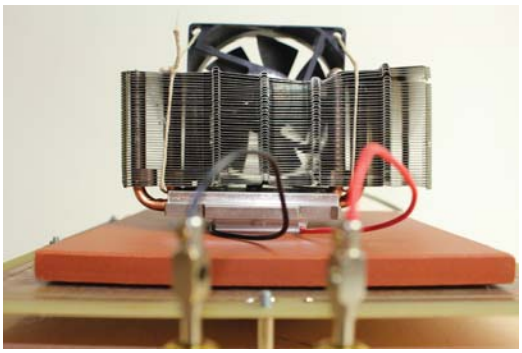

Fig. 5 Experiment in progress (side view): A two stage TEG mounted between a stone heated bed (hot side) and an aluminum heat sink with heat pipes and forced air cooling (cold side). Electrical connections visible in the foreground

VI. Benchmarking Bi_2Te_3 TEGs

As proof of concept, measurements were performed on a series of Bi_2Te_3 coolers (TECs) used as generators, with a experimental setup similar to Fig. 5. The goal is to demonstrate the usability of the presented solution

with commercial, off-the-shelf Peltier elements rather than dedicated application-specific thermoelectric generators as sold by Marlow, Nextreme, Micropelt and others. [35] The tested types are TEC1-12706 [18], CP2-12706 [28] and TEC2-19006 [11], which are available through third party distributors. A comparison of the physical and electrical properties of these TEGs is shown in Table I.

TABLE I
COMPARISON OF TEC1-12706, CP2-12706 AND TEC2-19006 TEG PROPERTIES

	TEC1-12706	CP2-12706	TEC2-19006
Semiconductors	Bi_2Te_3	Bi_2Te_3	Bi_2Te_3
Ceramics	Al_2O_3	Al_2O_3	Al_2O_3
Solder	BiSn	BiSn	BiSn
# thermocouples	127	127	190
Dimention (mm)	40 x 40	62 x 62	40 x 40
Thickness (mm)	3.9	4.572	6.4
Volume (cm^3)	6.24	17.57	10.24

The test setup allows two types of tests: A static test at a constant temperature gradient to measure the maximum power point (MPP) by performing a sweep and constructing a load line, and a dynamic test where the temperature is varied to determine the maximum power output in a specific temperature range.

A. Measuring MPP

To measure the MPP, as previously elaborated, the load is swept from short to open circuit by varying the channel impedance of the MOSFET between $R_{DS(on)} << 0.1\,\Omega$ (short circuit) and $R_{DS} >> 1\,\mathrm{M}\Omega$ (open circuit). For every impedance value, voltage-current pairs are measured and multiplied to obtain a power curve.

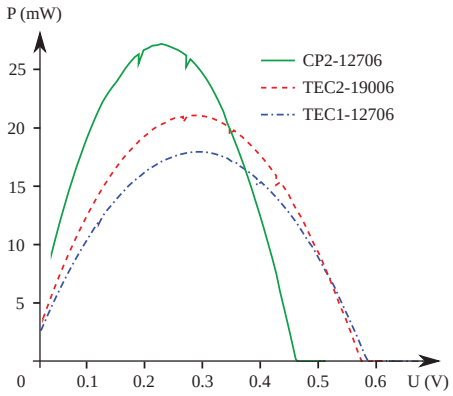

Fig. 6 Visualization of maximum power point (MPP) for 3 commercial TEGs. Note that the MPP is roughly equal to half the open circuit voltage V_{oc}

For a static test at 30 °C, the results are shown in Fig. 6 for the 3 TEGs. Parabolic power curves are characteristic for TEGs, and the MPP is found in $\frac{V_{oc}}{2}$. However, it should be noted that for consumer grade TEGs, the power output is not proportional to the TEG's volume, as shown in Table II.

TABLE II
POWER DENSITY ANALYSIS FOR THREE COMMERCIAL, CONSUMER GRADE TECS

	TEC1-12706	CP2-12706	TEC2-19006
P_{max} (ΔT = 30°C, mW)	17.9	27.2	21.1
Volume (cm^3)	6.24	17.57	10.24
Power density (mW/cm^3)	2.8	1.5	2.1

The differences can be attributed to variations in construction, thermal conductivity (i.e. differences in heat flux), mechanical composition, and optimization for higher or lower temperature differences. From datasheets alone, it is impossible to choose the most optimal TEG because the data does not allow for an adequate comparison. However, the presented test setup allows to mimic the target temperature difference at the intended environment of deployment, and enables the extraction of necessary data without much user interaction.

B. Measuring DC/DC Power Output

Even more important than estimating the MPP is making actual measurements of a TEG in conjunction with power conditioning circuitry. The low output voltage of a typical TEG prohibits powering an embedded electronic system directly, and a boost stage ("DC/DC step-up converter") is almost always necessary. Although any boost stage topology may be used as long as MPPT is enabled, the low cold start voltages tend to favour transformer based designs such as the LTC3108. Impedance matching through a transformer is difficult however, and the varying MPP in function of ΔT will pose a challenge to operate the TEG at high efficiency. This results in electrical conversion efficiencies below 30 % for cold start voltages below 45 mV. Alternatively, if a treshold between 250 mV and 400 mV is reached, cold starting a transformerless boost stage is possible. Several such solutions exist on the market: LTC3105 (250 mV cold start) from Linear Technology, BQ25504 (330 mV cold start) from Texas Instruments and AEM10940 (380 mV cold start) from E-peas. Unfortunately, quiescent power consumption as well as power switches in active mode result in a lower end-to-end power transfer than what may be estimated from DC/DC conversion losses alone. A second purpose of the presented test setup is measuring end-to-end power output *after* the DC/DC stage, aiming to provide embedded systems designs with power ratings that are directly usable to calculate the system's power budget [45] and its associated parameters [44].

Fig. 7 shows a comparison of the power generated by a TEC2-19006 under varying temperature differences. As expected, the highest output power is available when the maximum power point tracking is done externally by the test setup itself, rather than by a integrated maximum power point tracker. Although discrete MPPT systems exist [23], the choice is most often made for integrated MPPT controllers [10] to save cost, PCB area, and benefit from

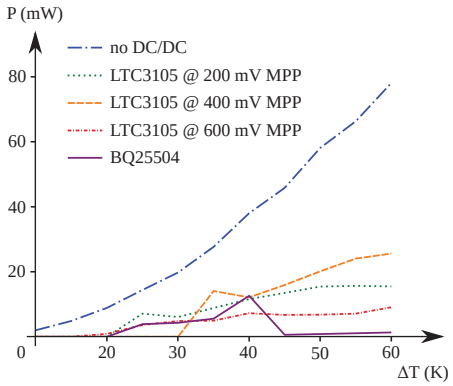

Fig. 7 DC/DC conversion stage effect on end-to-end power output for a TEC2-19006

better performance because of the typically higher switching frequencies. Unfortunately, the overhead caused by the DC/DC conversion stage is significant, as shown in Fig. 7, with overall conversion efficiencies below 50 %. Neither the LTC3105 nor the BQ25504 offer good performance, despite their difference in topology. The LTC3105 supports a fixed MPPT which can be set with an external bias resistor. Fig. 7 shows an average efficiency of ca. 40-50 % when set to 400 mV, implying an open circuit voltage for the TEG of around 800 mV. Unfortunately, as temperature changes, the MPP shifts accordingly, causing the LTC3105 to drift away from its MPP operation. Fortunately, as DC/DC conversion becomes more efficient as the voltage difference between input voltage and desired output voltage decreases, the performance hit can be slightly offset, resulting in an output power (orange in Fig. 7) that is surprisingly proportional to the input power (blue in Fig. 7) regardless of variations in temperature. For operation points too far from the actual MPP however, the output power converges to a maximum regardless of input power (green and red in Fig. 7). The test setup presented in this work can resolve this problem by measuring the MPP for a given operating environment beforehand, thus illustrating its usefulness for thermal embedded energy harvesting applications.

It has been observed that the BQ25504 performs worse in terms of end-to-end conversion efficiency than the LTC3105, despite being equipped with a dynamic MPPT instead of the static one. For dynamic MPPT, the MPP is set as a fraction of the open circuit voltage instead of a fixed point set by a bias resistor. Only at a temperature difference of 40 K does the BQ25504 meet the performance of the LTC3105, but never exceeds it. The higher power requirements of the dynamic MPPT logic itself could be a cause of this overhead, but differences in input impedance between LTC3105 and BQ25504 may also contribute to the performance difference. At higher temperature differences (corresponding to higher input voltages), the BQ25504's dynamic MPPT algorithm appears to lose track, causing the power output to drop off sharply beyond $\Delta T > 40$ K. This is unexpected for a device that is explicitly marketed as a boost converter for low power energy harvesting applications supported by TEGs.

As a final note, it is important to observe the cold start in Fig. 7. Neither converter is able to start up at temperature differences $\Delta T < 20$ K. For applications with passive cooled cold sides at room temperature (20 °), the limiting boundaries are around 0 °C and 40 °C. Immediate implications are the inherent incompatibility of the measured TEC2-19006 TEG for harvesting human body heat for example, as the temperature gradient is too low to start up any DC/DC power conversion stage.

VII. Future Work

The presented test setup is ready for use, and the authors do not see an expansion of its operational temperature ranges as a priority because the current maximum of 100 °C covers most of the environments typically targeted for energy harvesting applications, particularly domestic ones. However, possible synergies with photoelectric energy harvesting may be worth exploring since TEGs and solar cells require MPPT for optimal power transfer, which can be implemented following the same fundamentals. The DC/DC boost converters presented in this work are also compatible with both harvester types, allowing a seamless expansion of the original research scope to PV harvesting. Hybrid harvesting systems see increased attention in complementary balanced energy harvesting applications, and particularly solar and thermal energy harvesters are promising candidates to be combined.

A problem that deserves more attention is the accurate measurement of temperatures on both sides of the TEGs while being tested. This cannot be done indirectly (through heat flux) because the thermal characteristics of the TEG are unknown. However, temperature sensors – inserted between TEG and heat sink or hot plate – will disrupt heat flow and cause local hot spots due to their lower thermal conductivity. The homogeneous heat flux distribution is disturbed, leading to inconvenient side effects. Ideally, a method to measure the TEG temperature on either side should be implemented that causes minimal disruption of the heat flow. Miniaturization of the temperature sensor, or more sophisticated heating/cooling beds with integrated heat pipes are paths the authors think are worth investigating.

Finally, more measurements need to be done on a larger variety of different TEGs. For optimal convenience, benchmarking energy harvesters should not be something embedded system designers have to do when they start the design of a new application, rather, they should have approximate datasets at hand already. Filling up the IPEH database with data to support methodological design of energy harvesting powered embedded applications is the most important aspect. Unfortunately, due to large thermal inertia of heater, cooler and the DUT itself, temperature stabilization takes more time than could be considered convenient. Benchmarking all relevant parameters of a TEG may take up to a few hours, which is still too long to be really practical. The primary objective of the next design iteration will focus on reducing the time required to perform the necessary measurements.

VIII. Conclusion

This paper focused on the process of benchmarking the performance of TEGs to obtain their power characteristics. The aim of the presented work is to offer an easy and straight-forward method to determine the relevant parameters, independently from physical and/or electrical parameters of the TEG (thermal conductivity, semiconductor materials etc.). This has been accomplished with the design of a largely autonomous test setup allowing generic TEGs to be analysed to determine power output, maximum power point (MPP), short circuit current etc., parameters required to use them as energy harvesters in embedded electronic applications. The usability of the system has been demonstrated by measuring the performance of low cost commercial thermoelectric coolers for the consumer market: a TEC1-127006, TEC2-19006 and CP2-12706. An MPP of half of the open circuit voltage was measured for these TEGs, which is consistent with literature and supports the usability of the presented system. Finally, the necessary experiments were conducted to test the performance of DC/DC boost converters with integrated static or dynamic MPPT support. The presented results evidence a gap of over 50 % between input power and boost converter output power, independent of the chosen MPPT technique. The article concluded with remarks on practical selection criteria for TEGs and boost converters for embedded electronic applications.

Acknowledgment

The authors would like to thank the Flemish Agency for Innovation through Science and Technology (Agentschap voor Innovatie door Wetenschap en Technologie, IWT) for providing the funds that enabled this research in the context of the IPEH TETRA project. The prototype was generously sponsored by and manufactured in Fablab Brussels.

References

[1] Ahiska, R., Mamur, H., *A test system and supervisory control and data acquisition application with programmable logic controller for thermoelectric generators*, in Int. Conf. Renewable Energy (IREC), pp. 15 - 22, doi:10.1016/j.enconman.2012.05.010, 2012.

[2] Amatya, R., Ram, R. J., *Solar Thermoelectric Generator for Micropower Applications*, in J. of Electronic Materials, vol. 39, no. 9, pp. 1735 - 1740, doi:10.1007/s11664-010-1190-8, ISSN 1543-186X, 2010.

[3] Brown, S. R., Kauzlarich, S. M., Gascoin, F. et al., *$Yb_{14}MnSb_{11}$: New High Efficiency Thermoelectric Material for Power Generation*, in Chem. Mater., vol. 18, no. 7, pp. 1873 - 1877, doi:10.1021/cm060261t, 2006.

[4] Camargo, J. R., Costa de Oliveira, M. C., *Principles of Direct Thermoelectric Conversion, Heat Analysis and Thermodynamic Effects*, InTech, ISBN 978-953-307-585-3, doi:10.5772/20619, 2011.

[5] Cao, Z., Koukharenko, E., Tudor, M. J. et al., *Screen printed flexible Bi_2Te_3-Sb_2Te_3 based thermoelectric generator*, in J. Phys.: Conf. Ser., vol. 476, doi:10.1088/1742-6596/476/1/012031, 2013.

[6] Carmo, J. P., Antunes, J., Silva, M. F. et al., *Characterization of thermoelectric generators by measuring the load-dependence behavior*, in Measurement, vol. 44, no. 10, pp. 2194 - 2199, doi:10.1016/j.measurement.2011.07.015, 2011.

[7] Chen, J., Yan, Z., Wu, L., *The influence of Thomson effect on the maximum power output and maximum efficiency of a thermoelectric generator*, in J. Appl. Phys., vol. 79, no. 11, pp. 8823 - 8828, doi:10.1063/1.362507, 1996.

[8] Dughaish, Z. H., *Lead telluride as a thermoelectric material for thermoelectric power generation*, in Physica B: Condensed Matter, vol. 322, no. 1-2, pp. 205 - 223, doi:10.1016/S0921-4526(02)01187-0, 2002.

[9] Dziurdzia, P., *Modeling and Simulation of Thermoelectric Energy Harvesting Processes, Sustainable Energy Harvesting Technologies - Past, Present and Future*, InTech, ISBN 978-953-307-438-2, doi:10.5772/28530, 2011.

[10] Eakburanawat, J., Boonyaroonate, I., *Development of a thermoelectric battery-charger with microcontroller-based maximum power point tracking technique*, in Applied Energy, vol. 83, no. 7, pp. 687 - 704, doi:10.1016/j.apenergy.2005.06.004, 2006.

[11] Everredtronics Ltd., *Thermoelectric Module: TEC2-19006 Specifications*, datasheet, Rev. 1.01, online: http://www.everredtronics.com/files/TEC2-19006.pdf, 2015.

[12] Faraji, A. Y., Akbarzadeh, A., *Design of a Compct, Protable Test System for Thermoelectric Power Generator Modules*, in J. Electronic Materials, vol. 42, no. 7, pp. 1535 - 1541, ISSN 0361-5235, doi:10.1007/s11664-012-2314-0, 2013.

[13] Funahashi, R., Shikano, M., *$Bi_2Sr_2Co_2O_y$ whiskers with high thermoelectric figure of merit*, in Appl. Phys. Lett., vol. 81, pp. 1459 - 1461, doi:10.1063/1.1502190, 2002.

[14] Freunek, M., Müller, M., Ungan, T. et al., *New Physical Model for Thermoelectric Generators*, in J. of Electronic Materials, vol. 38, no. 7, pp. 1214 - 1220, doi:10.1007/s11664-009-0665-y, 2009.

[15] Ghamaty, S., Bass, J. C., Elsner, N. B., *Quantum well thermoelectric devices and applications*, in 22 Int. Conf. ICT Thermoelectrics, pp. 563 - 566, ISBN 0-7803-8301-X, doi:10.1109/ICT.2003.1287575, 2003.

[16] Goldsmid, H. J., *Bismuth Telluride and its Alloys as Materials for Thermoelectric Generation*, in Materials, vol. 7, no. 4, pp. 2577- 2592, doi:10.3390/ma7042577, 2014.

[17] Granger, P., Parvulescu, V. I., Kaliaguine, S. et al., *Perovskites and Related Mixed Oxides: Concepts and Applications*, John Wiley & Sons, ISBN 978-3-527-33763-7, 2016.

[18] Hebei I.T. Co., Ltd., *TEC1-12706 Thermoelectric Cooler*, datasheet, Rev. 2.03, online: http://www.hebeiltd.com.cn/peltier.datasheet/TEC1-12706.pdf, 2012.

[19] Heremans, J. P., Jovovic, V., Toberer, E. S. et al., *Enhancement of Thermoelectric Efficiency in PbTe by Distortion of the Electronic Density of States*, Science, vol. 321, no. 5888, pp. 554 - 557, 10.1126/science.1159725, 2008.

[20] Hu, L.-P., Zhu, T.-J., Wang, Y.-G. et al., *Shifting up the optimum figure of merit of p-type bismuth telluride-based thermoelectric materials for power generation by suppressing intrinsic conduction*, in NPGA Asia Materials, vol. 6, no. 2, e88, doi:10.1038/am.2013.86, 2014.

[21] Hsu, K. F., Loo, S., Guo, F. et al., *Cubic $AgPb_mSbTe_{2+m}$: Bulk Thermoelectric Materials with High Figure of Merit*, Science, vol. 303, no. 5659, pp. 818 - 821, doi:10.1126/science.1092963, 2004.

[22] Huang, M.-J., Yen, R.-H., Wang, A.-B., *The influence of the Thomson effect on the performance of a thermoelectric cooler*, in Int. J. of Heat and Mass Transfer, vol. 48, no. 2, pp. 413 - 418, doi:10.1016/j.ijheatmasstransfer.2004.05.040, 2005.

[23] Kim, S., Cho, S., Kim, N. et al., *A maximum power point tracking circuit of thermoelectric generators without digital controllers*, in IEICE Electronics Express, vol. 7, no. 10, pp. 1539 - 1545, doi:10.1587/elex.7.1539, 2010.

[24] Kristiansen, N. R., Nielsen, H. K., *Potential for Usage of Thermoelectric Generators on Ships*, in J. Electronic Materials, vol. 39, no. 9, pp. 1746 - 1749, ISSN 0361-5235, doi:10.1007/s11664-010-1189-1, 2010.

[25] Laird, I., Lovatt, H., Savvides, N. et al., *Comparative study of maximum power point tracking algorithms for thermoelectric generators*, in Power Engineering Conf. (AUPEC '08), pp. 1 - 6, ISBN 978-0-7334-2715-2, 2008.

[26] Manikandan, S., Kaushik, S. C., *Thermodynamic studies and maximum power point tracking in thermoelectric generator-thermoelectric cooler combined system*, in Cryogenics, vol. 67, pp. 52 - 62, doi:10.1016/j.cryogenics.2015.01.008, 2015.

[27] Massaguer, E., Massaguer, A., Montoro, J. et al., *Modeling analysis of longitudinal thermoelectric energy harvester in low temperature waste heat recovery applications*, in Applied Energy, vol. 140, pp. 184 - 195, doi:10.1016/j.apenergy.2014.12.005, 2015.

[28] Melcor Corporation, *CP2-127-06 Thermoelectric Cooler*, datasheet, Rev. 1.01, online: http://pdf.datasheetarchive.com/indexerfiles/Datasheets-UD3/DSAUD0046559.pdf, 2013.

[29] Montecucco, A., Buckle, J., Siviter, J. et al., *A New Test Rig for Accurate Nonparametric Measurement and Characterziation of Thermoelectric Generators*, in J. Electronic Materials, vol. 42, no. 7, pp. 1966 - 1973, ISSN 0361-5235, doi:10.1007/s11664-013-2484-4, 2013.

[30] Montecucco, A., Knox, A. R., *Maximum Power Point Tracking Converter Based on the Open-Circuit Voltage Method for Thermoelectric*

Generators, in IEEE Transactions on Power Electronics, vol. 30, no. 2, pp. 828 - 839, ISSN 0885-8993, doi:10.1109/TPEL.2014.2313294, 2014.
[31] Muller, E., Bruch, J. U., Schilz, J., *TE generator test facility for low resistance single elements*, in Proc. 17 Int. Conf. Thermoelectrics (ICT 98), pp. 441 - 444, ISBN 0-7803-4907-5, doi:10.1109/ICT.1998.740413, 1998.
[32] Niu, X., Yu, J., Wang, S., *Experimental study on low-temperature waste heat thermoelectric generator*, in J. Power Sources, vol. 188, no. 2, pp. 621 - 626, doi:10.1016/j.jpowsour.2008.12.067, 2009.
[33] Pean, R., Doluweera, G., Platonova, I., *Solid state lighting for the developing world: the only solution*, in Proc. SPIE 5941, 5 Int. Conf. Solid State Lighting, doi:10.1117/12.639718, 2005.
[34] Reddy, B. R., *Body Heat Powered Flashlight Using LTC3108*, in Int. J. of Engineering Research and Applications, vol. 4, no. 8, pp. 94 - 97, ISSN 2248-9622, 2014.
[35] Rossi, M., Rizzon, L., Fait, M., *Applications in Electronics Pervading Industry, Environment and Society: Self-powered Active Cooling System for High Performance Processors*, Springer International Publishing, vol. 351, pp. 25 - 33, ISBN 978-3-319-20226-6, doi:10.1007/978-3-319-20227-3_4, 2015.
[36] Salerno, D., *Ultralow voltage energy harvester uses thermoelectric generator for battery-free wireless sensors*, in J. Analog Innovation, vol. 20, no. 3, 2010.
[37] Shi, Y., Zhu, Z., Deng, Y. et al., *A real-sized three-dimensional numerical model of thermoelectric generators at a given thermal input and matched load resistance*, in Energy Conversion and Management, vol. 101, pp. 713 - 720, doi:10.1016/j.enconman.2015.06.020, 2015.
[38] Snyder, G. J., Ursell, T. S., *Thermoelectric Efficiency and Compatibility*, in Phys. Rev. Lett., vol. 91, no. 14, doi:10.1103/PhysRevLett.91.148301, 2003.
[39] Strasser, M., Aigner, R., Franosch, M. et al., *Miniaturized thermoelectric generators based on poly-Si and poly-SiGe surface micromachining*, in Sensors and Actuators A: Physical, vol. 97 - 98, pp. 535 - 542, doi:10.1016/S0924-4247(01)00815-9, 2002.
[40] Tan, J., Kalantar-zadeh, K., Wlodarski, W. et al., *Thermoelectric properties of bismuth telluride thin films deposited by radio frequency magnetron sputtering*, in Proc. SPIE 5836, Smart Sensors, Actuators, and MEMS II, 711, doi:10.1117/12.609819, 2005.
[41] Tritt, T. M., Subramanian, M. A., *Thermoelectric Materials, Phenomena, and Applications: A Bird's Eye View*, in MRS Bulletin, vol. 31, no. 3, pp. 188 - 198, doi:10.1557/mrs2006.44, 2006.
[42] Van Belle, D., *Ontwikkeling vna een modulair testopstelling voor onderzoek van laag vermogen indoor fotovoltaïsche cellen*, Master thesis, unpublished, Vrije Universiteit Brussel, Belgium, 2014.
[43] Van Belle, E., *Integrated low-cost sensorless BLDC motor controller using the BEMF on an FPGA*, Master thesis, unpublished, Vrije Universiteit Brussel, Belgium, 2015.
[44] Verbelen, Y., Braeken, A., Touhafi, A., *Parametrization of Ambient Energy Harvesters for Complementary Balanced Electronic Applications*, in Proc. SPIE 8763, Smart Sensors, Actuators, and MEMS VI, 87631U, doi:10.1117/12.2018490, 2013.
[45] Verbelen, Y., Braeken, A., Touhafi, A., *Towards a complementary balanced energy harvesting solution for low power embedded systems*, in Microsystem Technologies, vol. 20, no. 4, pp 1007-1021, doi:10.1007/s00542-014-2103-1, 2014.
[46] Verbelen, Y., Touhafi, A., *Resource Considerations for Durable Large Scale Renewable Energy Harvesting Applications*, in Proc. Int. Conf. Renewable Energy Research and Applications (ICRERA), pp. 401 - 406, doi:10.1109/ICRERA.2013.6749788, 2013.
[47] Ware, R. M., McNeill, D. J., *Iron disilicide as a thermoelectric generator material*, in Proc. IEEE, vol. 111, no. 1, pp. 178 - 182, doi:10.1049/piee.1964.0029, 1964.
[48] White, M. A., Colenbrander, K., Ronald, O. et al., *Generators that won't wear out*, in Mech. Eng., vol. 118, no. 2, pp. 92 - 96, 1996.
[49] Zaitsev, V. K., Fedorov, M. I., Gurieva, E. A. et al. *Highly effective* $Mg_2Si_{1-x}Sn_x$ *thermoelectrics*, in Phys. Rev. B., vol. 74, no. 4, doi:10.1103/PhysRevB.74.045207, 2005.
[50] Zou, H., Rowe, D. M., Min, G., *Growth of p- and n-type bismuth telluride thin films by co-evaporation*, in J. Crystal Growth, vol. 222, no. 1 - 2, pp. 82 - 87, doi:10.1016/S0022-0248(00)00922-2, 2001.

Yannick Verbelen graduated with a M.Sc degree in Industrial Engineering Sciences from the Vrije Universiteit Brussel, Belgium (VUB), with a specialization in embedded electronics. His research focuses on the application of renewable energy and energy harvesting technologies to extend the autonomy of electronic devices and to develop new, innovative solutions for existing problems using energy harvesting. He developed the theory for complementary balanced energy harvesting, and currently prepares a PhD on this topic. Other research topics include power electronics and mechatronics. He teaches courses on PCB design, analog and digital electronics and mechatronics at the Vrije Universiteit Brussel. Yannick is responsible for the coordination and development of prototyping technologies for electronics in Fablab Brussels, with an emphasis on PCB manufacturing.

Sam De Winne graduated with a M.Sc degree in Industrial Engineering Sciences from the Vrije Universiteit Brussel in 2014 with a specialization in informatics and communication technology (ICT). He coordinated research on ultrasonic sensing and ranging until 2015 when he shifted research emphasis towards sustainable and renewable technologies. Focussing on power path development for low power autonomous embedded devices, Sam developed methodologies for complementary balanced energy harvesters, harvester characterization and selection.

Niek Blondeel graduated with a M.Sc degree in Industrial Engineering Sciences from the Vrije Universiteit Brussel in 2014 with a specialization in embedded electronics. He published a thesis dissertation on pattern recognition algorithms for power budget characterization in wireless embedded systems powered by environmental energy in 2014, and continued this research until 2016 with a focus on indoor photovoltaics. He also designed and developed a high speed power meter for power measurements of embedded systems to optimize harvester and energy storage selection.

Ann Peeters has a background in Performance Arts and has earned credit in the Brussels social sector, focussing on engaging language learning techniques, as well as digital inclusion and coding programs. She has a university degree in Theatre studies, Teaching and Management, but is self-taught in 'Making'. Her passion for new technology and innovation led her to cordinate the Medialab and Fablab of the department of Design and Technology of the Erasmushogeschool Brussels. She has an unsatiable curiousity, and will ask annoying questions. She gets away with it, since her drive and enthouiasme work inspiring. She is fascinated by all forms of (interactive) storytelling and collaborative initiatives. Ann bikes her way through Brussels every day, volunteers locally for Coderdojo and Repair Caf. You could also bump into her on a swing dancing event or at a game-table. Ann loves Brussels for its diversity and unexpected encounters. Her hidden agenda involves more women in tech.

Ann Braeken obtained her MSc Degree in Mathematics from the University of Gent in 2002. In 2006, she received her PhD in engineering sciences from the KULeuven at the research group COSIC (Computer Security and Industrial Cryptography). In 2007, she became professor at Erasmushogeschool Brussel in the Industrial Sciences Department. Prior to joining the Erasmushogeschool Brussel, she worked for almost 2 years at a mangement consulting company BCG. Her current interests include cryptography, security protocols for sensor networks, secure and private localization techniques, and FPGA implementations.

Abdellah Touhafi obtained his bachelor's degree in Electronics, option: Computer systems at IHAM Antwerp. He has a Masters degree in Electronics from the VUB Brussels and a PhD in Applied Sciences: Scalable Run-Time Reconfigurable Computing Systems also at the VUB. He currently is a full time professor at the VUB and the leader of the Rapptor Lab.